ISSN 1990-7478, Biochemistry (Moscow) Supplement Series A: Membrane and Cell Biology, 2013, Vol. 7, No. 3, pp. 207–212. © Pleiades Publishing, Ltd., 2013.
Original Russian Text © A.V. Yakovlev, K.S. Koroleva, F.F. Valiullina, R.N. Khazipov, 2013, published in Biologicheskie Membrany, 2013, Vol. 30, No. 4, pp. 289–296.

ARTICLES

Resting Membrane Potential of the Rat Ventroposteriomedial Thalamic Neurons during Postnatal Development

A. V. Yakovlev[a], K. S. Koroleva[a], F. F. Valiullina[a], and R. N. Khazipov[a, b]

[a] *Kazan Federal University, Laboratory of Neurobiology, ul. Kremlevskaya, 18, Kazan, 420008 Russia;*
[b] *INSERM U901, 163 av. Lumini, Marseille, 13273 France;*
e-mail: roustem.khazipov@inserm.fr

Received February 22, 2013

Abstract—Resting membrane potential is a critical parameter determining tonic or bursting mode of the thalamic neurons. Previous studies using whole-cell recordings showed that immature ventroposteriomedial (VPM) and lateral geniculate thalamic neurons are strongly depolarized and have resting membrane potential near –50 mV. Yet, whole-cell recordings are associated with an introduction of the shunting conductance via the gigaseal that may lead to membrane depolarization in small neurons with high, in the gigaohm range, membrane resistance. Therefore, we have performed measurements of resting potential of VPM neurons in slices obtained from neonatal rats of postnatal days P2–P7 using cell-attached recordings of NMDA channels as voltage sensors. Because currents through the NMDA channels reverse near 0 mV, we assumed that the resting potential should equal the reversal potential of currents through NMDA channels in cell-attached recordings. Analysis of the current–voltage relationships of NMDA currents revealed that the resting potential in the immature VPM neurons is around –74 mV and that it does not change during the first postnatal week. This suggests that VPM neurons may operate in the bursting mode during the early postnatal period and support the oscillatory activity (spindle-like bursts) in the developing thalamocortical networks.

Keywords: membrane potential, neuron, patch-clamp, ion channels, NMDA, thalamus
DOI: 10.1134/S1990747813040089

Resting membrane potential is one of the fundamental features of a live cell. In neurons and other excitable cells membrane potential plays a key role in electrogenesis. Most ionic channels in cellular membranes are regulated by membrane potential. Membrane potential can directly modulate the probability of the channel activation, inactivation, and the return to the activable state. Among these channels are most sodium, calcium and potassium channels that open by membrane depolarization, HCN channels opened by hyperpolarization, as well as other channels controlled by various factors (for example, by neuromediators) but that are also modulated by the membrane potential. Therefore, information on the membrane potential value is crucial for comprehension of the functioning mechanisms of an excitable cell.

Measuring membrane potential is a challenging experimental task, however. Traditionally, various electrophysiological microelectrode techniques are employed, such as, for example, intracellular recording of membrane potential with sharp microelecrodes or recordings in whole-cell configuration of the patch-clamp method. However, these methods cause errors in the measurements, as in both cases the intracellular ion content is modified due to cell dialysis with the pipette-filling solution. Besides, the contact between cell membrane and electrode becomes a site of an artificial conductance (leakage) of about 500 MOhm in the case of sharp microelectrodes and of several GOhm in the case of patch-clamp recordings [1–5]. Addition of this non-selective ionic leakage conductance during intracellular or whole cell recordings should inevitably result in cell depolarization. Theoretically, this artifact will be maximal in cells with high input resistance [1, 6]. To avoid this disadvantage, alternative non-invasive ways of measurements of membrane potentials have been developed on the basis of patch-clamp recordings of the integral or single-channel currents in cell-attached configuration. In this case, cell membrane integrity is retained; dialysis does not take place, nor additional conductance is introduced. This method is based on the fact that membrane potential must be equal to the difference of the reversal potential of the current flowing through the known ion channels measured in the cell-attached configuration and the equilibrium potential of the currents through these channels. For this purpose, voltage-activated potassium channels [7, 8] and NMDA-channels [6, 9–13] have been used. The values of the membrane potential turned out to be much larger by absolute value than those obtained in whole-cell or perforated patch-clamp recordings. This difference was particularly ample in cells with high resistance of the membrane (lymphocytes [14], immature hyppoc-

ampal neurons of newly born rats [6]), which is consistent with the theoretical predictions.

Thalamus is the main interface between the external world and cortex in mammals [15, 16]. In particular, neurons of the ventroposteriomedial (VPM) thalamic nucleus receive the information from rat face, specifically, from vibrissae, and relay it to the somatosensory cortex. The values of the membrane potential of the relaying thalamic neurons determine their operating mode, that is, whether in the bursting or tonic manner the information is transmitted from sensory periphery to the cortex [17–20]. In the waking state, VPM neurons are depolarized (owing to the action of arousal neuromediators and hormons, such as noradrenaline and acetylcholine) and function in a tonic mode, which ensures a highly efficient, fast and stable transmission of the action potentials from sensor organs to the cortex. In the sleeping state depolarizing action of the waking mediators is absent, thus VPM neurons get hyperpolarized and switch to a bursting mode, so that the sensory input triggers an activity burst appearing as a series of action potentials. Such bursts of activity are not able to efficiently relay the sensory information to the brain cortex. Bursting and tonic modes of the thalamic neuron activity depend on the membrane potential and are mainly determined by the state of HCN- and low-threshold calcium channels, as well as by modulation of the activity of the reticular nucleus interneurones (owing to their hyperpolarization induced by acetylcholine) [20, 21]. The mode of activity of the thalamic neurons is also essential for generation of the thalamocortical rhythms, such as spindle oscillations in sleep phases 1 and 2 [18, 22–25]. Thus, membrane potential is an important parameter that determines functional properties and the – tonic or bursting mode of the thalamic neurons activity.

During early development, information from peripheral sensors (vibrissae) entering to the somatosensor cortex through thalamic VPM neurons is of great importance for the formation of topographic synaptic connections between VPM and cortical neurons that form the basis for so-called cortical maps [26, 27]. In rats these maps are formed within the first week after birth. This period is also characterized by unique oscillatory activity patterns in thalamocortial neuronal networks, in which the role of pacemakers of early oscillations is played by thalamic neurons [28–33]. Analysis of the reponses evoked in sensory cortex by sensor stimuli suggests bursting type of the activity of the thalamic neurons. At the same time, patch-clamp whole-cell recordings performed from rat VPM neurons during the first week after birth revealed that neurons are depolarized (resting membrane potential is about –50 mv) and are unable to generate low-theshold spikes and bursting activity in response to stimulation of the internal capsule or to depolarizing steps [34]. Similar data were also obtained in the neurons of visual relay lateral geniculate thalamus [35]. This suggested that immature thalamic neurons are depolarized and cannot therefore support busting mode of activity required for generation of certain oscillatory rhythms, for example, sleep spindles. On the other hand, VPM neurons are characterized by high resistance of the cell membrane. This raises a question of whether the observed depolarized state of the immature VPM neurons is a true age-related phenomenon or the values of membrane potentials measured by patch-clamp whole-cell technique are underestimated due to the induced leakage mentioned above. To answer this question, we recorded the activity of NMDA channels in cell-attached configuration and from these data estimated resting potentials of the VPM neurons of newly born rats.

MATERIALS AND METHODS

Experiments were carried out on slices of rat thalamic VPM nucleus on the first postnatal week (postnatal days (P) 2–7). All experimental procedures were conducted in accordance with the ethic norms on the human care of experimental animals accepted in Kazan Federal University and at INSERM. Before experiments, animals were anesthetized by isofluran (4%) or were subjected to cryoanesthesia. After isolation, the rat brains were placed into a cooled oxigenated artificial cerebrospinal fluid (ACSF) of the following composition (in mM): NaCl, 126; KCl, 3.5; $CaCl_2$ 2.0, $MgCl_2$ 1.3, $NaHCO_3$ 25, NaH_2PO_4 1.2, and glucose, 11 (pH 7.4). Horizontal 400-μm-thick slices of the brain were cut using vibroslicer HM 650 V (Microm International, Germany). Slices containing VPM were placed into oxigenated ACSF and incubated for at least 1 h at room temperature before recordings. During recordings, slices with VPM were fully immersed in a superfusing solution in a standard chamber and were constantly superfused with ACSF (30–32°C) at a rate of 2–3 ml/min.

Patch-clamp recordings were carried out on VPM neurons with visual control by means of microscope Axio Examiner A1 (400×, Carl Zeiss, Germany), using differential interference contrast. Patch-clamp amplifier Axopatch 200B (Axon Instruments, USA) was employed for the signal recordings; the gain was 50 mV/pA and the bandpath, 0–2 kHz. Patch-pipettes were prepared from borosilicate glass capillaries with outer and inner diameter of 1.5 and 0.86 mm, respectively (GC150F-15, Clark Electromedical Instruments, UK). For records of single NMDA channels, pipettes were filled with nominally Mg-free ACSF containing NMDA (10 μM) and glycine (10 μM). In each experiment the activity of NMDA channels was recorded at different voltages on the patch-pipette, varying from 20 to –120 mV in a stepwise manner, with a step of 10–20 mV. Electrophysiological signals were digitized at a frequency of 10 kHz using AD converter Digidata 1440 (Axon Instruments, USA) and further analyzed using Axon Software Package and

Origin 7.5 (Microcal Software, USA). Detection of the opening of single NMDA channels and analysis of the single-channel current amplitudes was performed by means of Axon Software Package after additional filtration of the singnals, as described earlier [36].

Group data are presented as mean ± standard error. Statistical analysis of parametric data was performed using Student's *t*-test at a significance level of $p < 0.05$.

RESULTS AND DISCUSSION

In this work we have measured resting membrane potentials in VMP neurons of rats during the first postnatal week by means of NMDA-channel recordings in cell-attached configuration. This approach is based on the fact that the reversial potential of the non-selective cationic NMDA channels is close to 0 mV [36]; therefore, in cell-attached configuration the currents through the NMDA channels should reverse at the pipette voltage equal to the cell resting potential. Earlier this technique was successfully applied for measurements of membrane potentials of rat hyppocampal and neocortical neurons, as well as of cortical neurons in human brain, using samples obtained during surgical operations [6, 9–13].

Examples of activity of single NMDA channels recorded from a VMP neuron of a 2-day-old rat are given in Fig. 1. At the pipette voltage equal to 0 mV, single NMDA channel openings were manifested as transient, 2–5-ms long steps of inward current with amplitude of 4.9 ± 0.3 pA ($n = 17$ cells; age of animals, from 2 to 7 days after birth). It should be noted that in cell-attached configuration currents are directed opposite to those recorded intracellularly; therefore, inward currents in cell-attached mode are upward. Hyperpolarization of the recorded patch of membrane by applying positive voltage to the patch-pipette, increased the amplitude of the currents through the NMDA channels, while the patch depolarization during recordings with negative voltages at the pipette lead to the current amplitude decrease. Besides, at the negative pipette voltages the open times of the NMDA channels increased and the closed time decreased that likely reflects a relieve of the magnesium block of NMDA channels owing to residual Mg^{2+} ions that are present in micromolar concentrations even in nominally Mg^{2+}-free solutions. At a considerable depolarization of the patched membrane, currents through the NMDA channels were indistinguishable from the baseline level; at further depolarization, the recorded currents reversed, that is, they became outwardly directed. It is of note that in most recordings, depolarization of the membrane to an intermediate level above the reversial potential of NMDA channels (about −50 mV) and also upon their reversial, evoked the opening of other type of channels that were characterized by outward direction with an amplitude increasing with depolarization. Most likely, these were voltage-activated potassium channels; they were excluded from the analysis of the NMDA-channel activity. Considerable depolarization resulting in a massive opening of these presumably potassium channels markedly increased the baseline noise and hindered the detection of the NMDA channels. Considering this contamination of recordings by non-NMDA channels and the intracellular Mg-induced block of the NMDA channels that accounts for nonlinear deviation of the current–voltage relationship for the outward currents, we restricted the analysis of the voltage dependence of the currents through

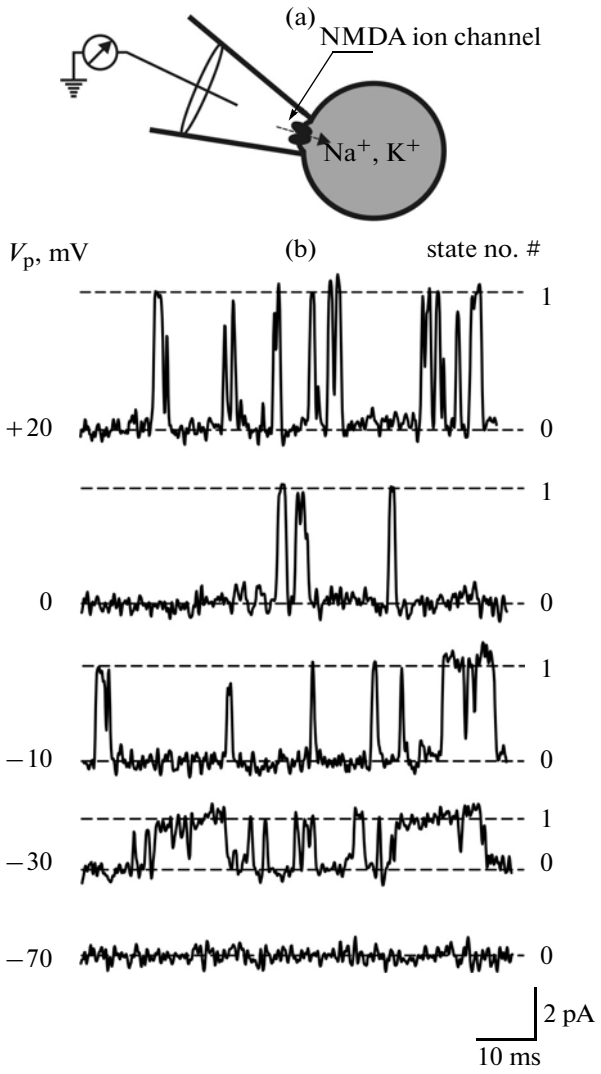

Fig. 1. Measurements of resting potentials of thalamic cells by cell-attached patch-clamp technique using NMDA channels as the membrane potential sensors. (a) Experimental design. Cell-attached recordings of the currents through single NMDA channels from a VPM neuron are performed with a patch-pipette filled with a solution containing NMDA and glycine. (b) Examples of current traces through single NMDA channels at various voltages on the patch electrode (V_p). Closed (0) and open (1) states of the channels are shown by dotted lines.

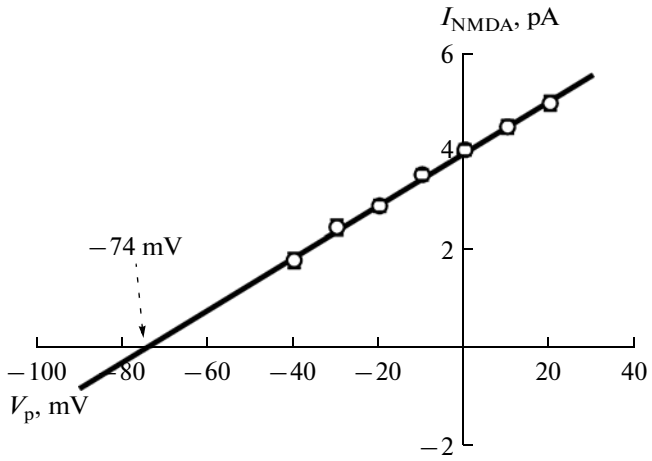

Fig. 2. Current–voltage relationships for single NMDA channels. Amplitude of the currents through NMDA channels is plotted as a function of the voltage on the patch electrode (*V*p), and the obtained curve is approximated with a linear function. As the currents through the NMDA channels reverse at membrane potential of about zero mV, the reversal potential of the NMDA channels in cell-attached configuration (shown by an *arrow*) corresponds to the cell resting potential. The plot is based on the recordings of NMDA channels from four VPM neurons of 7-day-old rats. ìÂ ? mV.

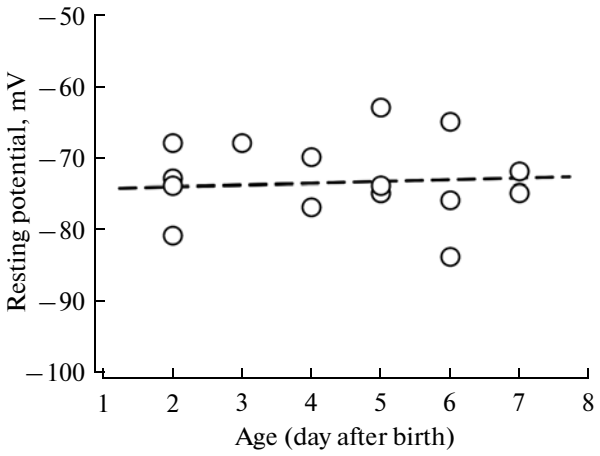

Fig. 3. Age-dependence of resting potentials of VPM neurons. Each *symbol* on the plot corresponds to a mean value of a membrane potential of one cell. *Dotted line* designates linear regression of the age-dependence of the membrane potential ($R = 0.072 \pm 5.18$; $P = 0.36$).

NMDA channels to the voltage range on the patch electrode from 20 to −50 mV.

Based on the measurements of the amplitudes of single-channel currents flowing through the NMDA channels at various voltages applied to the electrode, current–voltage plots were constructed for the NMDA currents of each cell (Fig. 2). In all experiments the current–voltage relationships were satisfactorily approximated by linear function ($R = 0.998 \pm 0.006$; $n = 17$; $P = 0.001$). Single-channel conductance of the NMDA channels varied from 46 to 81 pS (mean conductance, 63 ± 3 pS). Currents reversed at the electrode voltage of −74 ± 1 mV, ranging from −63 to −84 mV in 17 cells. As was discussed earlier, these values correspond to the resting membrane potentials in VPM neurons. In Fig. 3 the membrane potential values of the VPM neurons are plotted versus the animal age (2–7 day after birth). No statistically significant relations between the age and membrane potential was revealed within this postnatal period ($n = 17$ cells; $P = 0.36$).

Thus, using a non-invasive method of membrane potential measurements employing the NMDA-channels as membrane potential sensors in the cell-attached configuration of the patch-clamp recordings, we found that the membrane of VPM neurons is much more hyperpolarized than it appeared in experiments using whole-cell configuration of the patch-clamp technique [34, 37]. The reasons for this difference in the membrane potential values obtained by the two methods are most likely related with the leakage phenomenon that considerably alters this parameter, particularly in neurons with high membrane resistance. This phenomenon was described earlier in hippocampal neurons of newborn rats. It was shown in particular that the membrane potential values obtained in the whole-cell configuration clearly correlated with the giga-seal resistance (the lower the resistance, the more depolarized is the membrane) and with the cell membrane resistance (the higher the resistance, the more are the membrane potential values are shifted towards depolarization) [6]. Moreover, simultaneous measurements from the same neurons by both methods indicated that membrane is strongly hyperpolarized when the membrane potential is estimated by means of cell-attached recordings. However, after the formation of whole-cell configuration on the same cell by another electrode, membrane depolarized considerably, and the membrane potential values recorded by the electrode in the whole-cell configuration matched those obtained by current–voltage relationships of the NMDA channels [12]. Hence, the membrane potential values of the neonate (2–7 day old) rat VPM neurons obtained earlier using whole-cell recordings are underestimated due to the measurement error, unavoidable for this recording method applied to small-size neurons with high membrane resistance, and they do not reflect developmental phenomenon, as was previously suggested.

Our findings suggest that the functional properties of the VPM neurons during early ontogenesis, as well as their role in sensory signal processing and generation of the early activity patterns in the developing thalamocortical networks should be revised. It was suggested previously that once VPM neurons are depolarized (resting potentials are about −50/−55 mV), then Ca^{2+} channels involved in the generation of low-threshold (with activation threshold of

about −70 mV) calcium spikes (LTS) are inactivated; moreover, upon depolarization from this membrane potential the VPM cells are able to support only tonic activity with a considerable delay after the beginning of depolarization [34]. The VPM neurons acquired the ability to generate LTS in response to application of depolarizing current pulses only if the negative hyperpolarizing current was injected to support sufficiently negative potential on the membrane. Our data show that the real membrane potential of the VPM neurons of newly born rats is about −74 mV; this suggest that in the resting state the low-threshold calcium channels are activable. Hence, depolarization of neurons should evoke activation of LTS and thus support the bursting mode of activity in the VPM neurons. This corresponds to the bursting activity triggered in the thalamic VPM nucleus upon stimulation of the sensory input in intact animals in vivo, as well as to the bursting type of the sensory responses recorded in somatosensory and visual cortex during the early stages of development [28–31, 33, 38]. Resting potential may also promote activation of H-currents that are activated upon hyperpolarization (for example, as a result of activition of GABAergic synapses from reticular nucleus) and are involved in the LTS activation and bursting activity during the decay of the inhibitory potentials [39, 40]. These processes play a key role in generation of the network activity patterns, such as, for example, sleep spindles [41, 42]. It has been thought for a long time that sleep spindles appear quite late, at the end of the second postnatal week [43]. However, it was shown recently that spindle-like bursts can be recorded in the rat cortex already during the first postnatal week; these bursts share many common features with sleep spindles of the adult animals (although some differences do exist) [28]. This agrees with our data on the hyperpolarized state of the thalamic neurons as well. Thus, our results suggest a revision of a number of properties of VPM neurons that determine the mode of the information transmission from sensory periphery to the cortex and their involvement in the generation of the network events during the early postnatal period.

ACKNOWLEDGMENTS

The work was supported by the grant of the Russian Federation government for leading scientists (project no. 11.G34.31.0075) and by ANR (ANR-09-MNPS-006) and FRM (DEQ20110421301).

REFERENCES

1. Barry P.H., Lynch J.W. 1991. Liquid junction potentials and small cell effects in patch-clamp analysis. *J. Membr. Biol.* **121**, 101–117.
2. Hamill O.P., Marty A., Neher E., Sakmann B., Sigworth F.J. 1981. Improved patch-clamp techniques for high-resolution current recording from cell-free membrane patches. *Pflüg. Arch.* **391**, 85–100.
3. Spruston N., Johnston D. 1992. Perforated patch-clamp analysis of the passive membrane properties of three classes of hippocampal neurons. *J. Neurophysiol.* **67**, 508–529.
4. Staley K.J., Otis T.S., Mody I. 1992. Membrane properties of dentate gyrus granule cells: comparison of sharp microelectrode and whole-cell recordings. *J. Neurophysiol.* **67**, 1346–1358.
5. Velumian A.A., Zhang L., Pennefather P., Carlen P.L. 1997. Reversible inhibition of I_K, I_{AHP}, I_h and I_{Ca} currents by internally applied gluconate in rat hippocampal pyramidal neurones. *Pflüg. Arch.* **433**, 343–350.
6. Tyzio R., Ivanov A., Bernard C., Holmes G.L., Ben Ari Y., Khazipov R. 2003. Membrane potential of CA3 hippocampal pyramidal cells during postnatal development. *J. Neurophysiol.* **90**, 2964–2972.
7. Fricker D., Verheugen J.A., Miles R. 1999. Cell-attached measurements of the firing threshold of rat hippocampal neurones. J. Physiol. 517, 791–804.
8. Verheugen J.A., Fricker D., Miles R. 1999. Noninvasive measurements of the membrane potential and GABAergic action in hippocampal interneurons. *J. Neurosci.* **19**, 2546–2555.
9. Khazipov R., Leinekugel X., Khalilov I., Gaïarsa J.-L., Ben-Ari Y. 1997. Synchronization of GABAergic interneuronal network in CA3 subfield of neonatal rat hippocampal slices. *J. Physiol.* (Lond). **498** 763–772.
10. Leinekugel X., Medina I., Khalilov I., Ben-Ari Y., Khazipov R. 1997. Ca^{2+} oscillations mediated by the synergistic excitatory actions of $GABA_A$ and NMDA receptors in the neonatal hippocampus. *Neuron.* **18**, 243–255.
11. Tyzio R., Cossart R., Khalilov I., Minlebaev M., Hubner C.A., Represa A., Ben Ari Y., Khazipov R. 2006. Maternal oxytocin triggers a transient inhibitory switch in GABA signaling in the fetal brain during delivery. *Science.* **314**, 1788–1792.
12. Tyzio R., Minlebaev M., Rheims S., Ivanov A., Jorquera I., Holmes G.L., Zilberter Y., Ben Ari Y., Khazipov R. 2008. Postnatal changes in somatic gamma-aminobutyric acid signalling in the rat hippocampus. *Eur. J. Neurosci.* **27**, 2515–2528.
13. Tyzio R., Khalilov I., Represa A., Crepel V., Zilberter Y., Rheims S., Aniksztejn L., Cossart R., Nardou R., Mukhtarov M., Minlebaev M., Epsztein J., Milh M., Becq H., Jorquera I., Bulteau C., Fohlen M., Oliver V., Dulac O., Dorfmuller G., Delalande O., Ben-Ari Y., Khazipov R. 2009. Inhibitory actions of the gamma-aminobutyric acid in pediatric Sturge–Weber syndrome. *Ann. Neurol.* **66**, 209–218.
14. Verheugen J.A., Vijverberg H.P., Oortgiesen M., Cahalan M.D. 1995. Voltage-gated and Ca^{2+}-activated K^+ channels in intact human T lymphocytes. Noninvasive measurements of membrane currents, membrane potential, and intracellular calcium. *J. Gen. Physiol.* **105**, 765–794.
15. Jones E.G. 2009. Synchrony in the interconnected circuitry of the thalamus and cerebral cortex. *Ann. N.Y. Acad. Sci.* **1157**, 10–23.
16. Castro-Alamancos M.A. 2004. Dynamics of sensory thalamocortical synaptic networks during information processing states. *Prog. Neurobiol.* **74**, 213–247.

17. Deschenes M., Roy J.P., Steriade M. 1982. Thalamic bursting mechanism: an inward slow current revealed by membrane hyperpolarization. *Brain Res.* **239**, 289–293.

18. Llinas R.R., Steriade M. 2006. Bursting of thalamic neurons and states of vigilance. *J. Neurophysiol.* **95**, 3297–3308.

19. Ramcharan E.J., Gnadt J.W., Sherman S.M. 2000. Burst and tonic firing in thalamic cells of unanesthetized, behaving monkeys. *Vis. Neurosci.* **17**, 55–62.

20. McCormick D.A., Bal T. 1997. Sleep and arousal: thalamocortical mechanisms. *Annu. Rev. Neurosci.* **20**, 185–215.

21. McCormick D.A. 1989. Cholinergic and noradrenergic modulation of thalamocortical processing. *Trends Neurosci.* **12**, 215–221.

22. McCormick D.A. 2002. Cortical and subcortical generators of normal and abnormal rhythmicity. *Int. Rev. Neurobiol.* **49**, 99–114.

23. Huguenard J.R., McCormick D.A. 2007. Thalamic synchrony and dynamic regulation of global forebrain oscillations. *Trends Neurosci.* **30**, 350–356.

24. Steriade M. Llinas R.R. 1988. The functional states of the thalamus and the associated neuronal interplay. *Physiol. Rev.* **68**, 649–742.

25. Steriade M., Contreras D., Amzica F. 1994. Synchronized sleep oscillations and their paroxysmal developments. *Trends Neurosci.* **17**, 199–208.

26. Van der Loos H., Woolsey T.A. 1973. Somatosensory cortex: structural alterations following early injury to sense organs. *Science.* **179**, 395–398.

27. Erzurumlu R.S., Gaspar P. 2012. Development and critical period plasticity of the barrel cortex. *Eur. J. Neurosci.* **35**, 1540–1553.

28. Khazipov R., Sirota A., Leinekugel X., Holmes G.L., Ben Ari Y., Buzsaki G. 2004. Early motor activity drives spindle bursts in the developing somatosensory cortex. *Nature.* **432**, 758–761.

29. Khazipov R., Luhmann H.J. 2006. Early patterns of electrical activity in the developing cerebral cortex of humans and rodents. *Trends Neurosci.* **29**, 414–418.

30. Colonnese M.T., Kaminska A., Minlebaev M., Milh M., Bloem B., Lescure S., Moriette G., Chiron C., Ben-Ari Y., Khazipov R. 2010. A conserved switch in sensory processing prepares developing neocortex for vision. *Neuron.* **67**, 480–498.

31. Minlebaev M., Ben-Ari Y., Khazipov R. 2007. Network mechanisms of spindle-burst oscillations in the neonatal rat barrel cortex *in vivo*. *in vivo*. *J. Neurophysiol.* **97**, 692–700.

32. Minlebaev M., Ben Ari Y., Khazipov R. 2009. NMDA receptors pattern early activity in the developing barrel cortex *in vivo*. *Cereb. Cortex.* **19**, 688–696.

33. Minlebaev M., Colonnese M., Tsintsadze T., Sirota A., Khazipov R. 2011. Early gamma oscillations synchronize developing thalamus and cortex. *Science.* **334**, 226–229.

34. Warren R.A., Jones E.G. 1997. Maturation of neuronal form and function in a mouse thalamo-cortical circuit. *J. Neurosci.* **17**, 277–295.

35. Ramoa A.S., McCormick D.A. 1994. Developmental changes in electrophysiological properties of LGNd neurons during reorganization of retinogeniculate connections. *J. Neurosci.* **14**, 2089–2097.

36. Khazipov R., Ragozzino D., Bregestovski P. 1995. Kinetics and Mg^{2+} block of N-methyl-*D*-aspartate receptor channels during postnatal development of hippocampal CA3 pyramidal neurons. *Neuroscience.* **69**, 1057–1065.

37. Ramoa A.S. McCormick D.A. 1994. Developmental changes in electrophysiological properties of LGNd neurons during reorganization of retinogeniculate connections. *J. Neurosci.* **14**, 2089–2097.

38. Yang J.W., An S., Sun J.J., Reyes-Puerta V., Kindler J., Berger T., Kilb W., Luhmann H.J. 2012. Thalamic network oscillations synchronize ontogenetic columns in the newborn rat barrel cortex. *Cereb. Cortex.* [Epub ahead of print]

39. McCormick D.A., Pape H.C. 1990. Properties of a hyperpolarization-activated cation current and its role in rhythmic oscillation in thalamic relay neurones. *J. Physiol.* (Lond). **431**, 291–318.

40. Evrard A., Ropert N. 2009. Early development of the thalamic inhibitory feedback loop in the primary somatosensory system of the newborn mice. *J. Neurosci.* **29**, 9930–9940.

41. Kandel A., Buzsaki G. 1997. Cellular-synaptic generation of sleep spindles, spike-and-wave discharges, and evoked thalamocortical responses in the neocortex of the rat. *J. Neurosci.* **17**, 6783–6797.

42. Steriade M. 1995. Thalamic origin of sleep spindles: Morison and Bassett (1945). *J. Neurophysiol.* **73**, 921–922.

43. Jouvet-Mounier D., Astic L., Lacote D. 1970. Ontogenesis of the states of sleep in rat, cat, and guinea pig during the first postnatal month. *Developmental Psychobiology.* **2**, 216–239.

Translated by A. Dunina-Barkovskaya

SPELL: 1. Starkov